

OVERVIEW OF THE ATLAS PROJECT

R. J. Trainor, W. M. Parsons, E. O. Ballard, R. R. Bartsch, J. F. Benage, G. A. Bennett, R. L. Bowers, D. W. Bowman, J. H. Brownell, J. C. Cochrane, H. A. Davis, C. A. Ekdahl, R. D. Fulton, R. F. Gribble, J. R. Griego, J. Guzik, M. E. Jones, W. B. Hinckley, K. W. Hosack, R. J. Kasik, R. Keinigs, H. Lee, E. A. Lopez, I. R. Lindemuth, M. D. Monroe, R. W. Moses, D. Oro, S. A. Ney, D.D. Pierce, D. Platts, W. A. Reass, R. E. Reinovsky, G. Rodriguez, H. R. Salazar, G. M. Sandoval, D. W. Scudder, M. Sheppard, J. S. Shlachter, A. Taylor, M. C. Thompson, G. A. Valdez, R. G. Watt, and G. A. Wurden

*Los Alamos National Laboratory
Los Alamos, New Mexico 87545*

Abstract

Atlas is a high energy pulsed power facility under development at Los Alamos National Laboratory to perform high energy-density experiments in support of the Department of Energy's stockpile stewardship responsibility. Its design is optimized for materials properties and hydrodynamics experiments under extreme conditions. Atlas will be operational in late-1999 and is designed to provide 100 shots per year. The Atlas capacitor bank design consists of a 36-MJ array of 240-kV Marx modules. The system is designed to deliver a peak current of 40-50 MA with a 4-5 μ s risetime. The Marx modules are designed to be reconfigured to a 480-kV configuration, if needed, for opening switch development. The bank is resistively damped to limit fault currents and capacitor voltage reversal. The system is configured for very low-inductance operation (total inductance \sim 10 nH) to rapidly implode heavy liner loads. An experimental program for testing and certifying prototype components is currently underway. For many applications the Atlas liner will be a nominal 70g aluminum cylinder. Using composite inner layers and a variety of interior target designs, a wide variety of experiments in \sim cm³ volumes may be performed. These include shock compression experiments up to \sim 3 TPa (30 Mbar), quasi-adiabatic compressions up to 6-fold compression and pressures above 10 TPa, hydrodynamic instability studies in nonlinear and turbulent regimes over multi-cm propagation lengths, experiments with dense plasmas in the so-called high-gamma regime, studies of materials response at very high strains and strain rates, and materials studies in ultrahigh magnetic fields (above 10³ T).

Introduction

The Atlas project at Los Alamos is an element of a strategic response to the changing requirements being placed on Department of Energy (DOE) Defense Programs (DP). These requirements include the Presidential call¹ to ensure the safety and reliability of US nuclear weapons without underground testing. DOE and the national laboratories will continue their responsibility for maintenance, surety, and reliability of the Nation's stockpile.

High energy-density physics experiments require various environments to successfully support necessary weapons-related experiments. Both pulsed-power and high-intensity laser capabilities are called out in the DOE/DP Stockpile Stewardship and Management Program². Atlas will be the first of several new facilities constructed to support this Program. Atlas will also be used to perform basic research experiments³ to support science and technology development.

Report Documentation Page

Form Approved
OMB No. 0704-0188

Public reporting burden for the collection of information is estimated to average 1 hour per response, including the time for reviewing instructions, searching existing data sources, gathering and maintaining the data needed, and completing and reviewing the collection of information. Send comments regarding this burden estimate or any other aspect of this collection of information, including suggestions for reducing this burden, to Washington Headquarters Services, Directorate for Information Operations and Reports, 1215 Jefferson Davis Highway, Suite 1204, Arlington VA 22202-4302. Respondents should be aware that notwithstanding any other provision of law, no person shall be subject to a penalty for failing to comply with a collection of information if it does not display a currently valid OMB control number.

1. REPORT DATE JUN 1997	2. REPORT TYPE N/A	3. DATES COVERED -
4. TITLE AND SUBTITLE Overview Of The Atlas Project		5a. CONTRACT NUMBER
		5b. GRANT NUMBER
		5c. PROGRAM ELEMENT NUMBER
6. AUTHOR(S)	5d. PROJECT NUMBER	
	5e. TASK NUMBER	
	5f. WORK UNIT NUMBER	
7. PERFORMING ORGANIZATION NAME(S) AND ADDRESS(ES) Los Alamos National Laboratory Los Alamos, New Mexico 87545		8. PERFORMING ORGANIZATION REPORT NUMBER
9. SPONSORING/MONITORING AGENCY NAME(S) AND ADDRESS(ES)		10. SPONSOR/MONITOR'S ACRONYM(S)
		11. SPONSOR/MONITOR'S REPORT NUMBER(S)

12. DISTRIBUTION/AVAILABILITY STATEMENT
Approved for public release, distribution unlimited

13. SUPPLEMENTARY NOTES
See also ADM002371. 2013 IEEE Pulsed Power Conference, Digest of Technical Papers 1976-2013, and Abstracts of the 2013 IEEE International Conference on Plasma Science. Held in San Francisco, CA on 16-21 June 2013. U.S. Government or Federal Purpose Rights License.

14. ABSTRACT
Atlas is a high energy pulsed power facility under development at Los Alamos National Laboratory to perform high energy-density experiments in support of the Department of Energys stockpile stewardship responsibility. Its design is optimized for materials properties and hydrodynamics experiments under extreme conditions. Atlas will be operational in late-1999 and is designed to provide 100 shots per year. The Atlas capacitor bank design consists of a 36-MJ array of 240-kV Marx modules. The system is designed to deliver a peak current of 40-50 MA with a 4-5 ps risetime. The Marx modules are designed to be reconfigured to a 480-kV configuration, if needed, for opening switch development. The bank is resistively damped to limit fault currents and capacitor voltage reversal. The system is configured for very low-inductance operation (total inductance - 10 nH) to rapidly implode heavy liner loads. An experimental program for testing and certifying prototype components is currently underway. For many applications the Atlas liner will be a nominal 70g aluminum cylinder. Using composite inner layers and a variety of interior target designs, a wide variety of experiments in -cm³ volumes may be performed. These include shock compression experiments up to -3 TPa (30 Mbar), quasi-adiabatic compressions up to 6-fold compression and pressures above 10 TPa, hydrodynamic instability studies in nonlinear and turbulent regimes over multi-cm propagation lengths, experiments with dense plasmas in the so-called highgamma regime, studies of materials response at very high strains and strain rates, and materials studies in ultrahigh magnetic fields (above 103T).

15. SUBJECT TERMS

16. SECURITY CLASSIFICATION OF:			17. LIMITATION OF ABSTRACT SAR	18. NUMBER OF PAGES 10	19a. NAME OF RESPONSIBLE PERSON
a. REPORT unclassified	b. ABSTRACT unclassified	c. THIS PAGE unclassified			

Standard Form 298 (Rev. 8-98)
Prescribed by ANSI Std Z39-18

Table I. Atlas parameters

Stored energy	36 MJ
Energy in load	6-10 MJ
Discharge voltage	240 kV
Peak current	40-50 MA
Current risetime	4 μ s
Total inductance	10 nH

Atlas will generate high energy density conditions by discharging 40-50 MA currents into a centrally located, cylindrical liner. Near the liner, the current density and associated magnetic fields dramatically increase. The interaction of the current and magnetic field produces Lorentz forces which implode the cylindrical liner. Lightweight liners are designed to pinch on axis, converting kinetic energy into soft x-rays; this forms the basis of experimental programs at Saturn⁴ and PBFA-Z.⁵ The heavy liners designed

for Atlas can be used to either compress sample materials to high pressures, or when driven into a central target, produce extremely high shock pressures for hydrodynamic experiments. Nominal design and operating parameters for Atlas are listed in Table 1.

Capacitor Bank Requirements and Design

Atlas must be flexible in order to accommodate a wide variety of weapons physics and basic research experiments. Other requirements for the facility include: (1) maximizing the radial and axial diagnostic access around the target chamber, (2) a machine reliability of 95% or greater, (3) a repetition rate of 100 shots per year, and (4) a machine lifetime of 1000 tests at full voltage. Finally, the facility must include full support services for users including data analysis, film processing, and planning and coordination areas. A design view of the Atlas capacitor bank and target chamber is shown in Fig. 1.

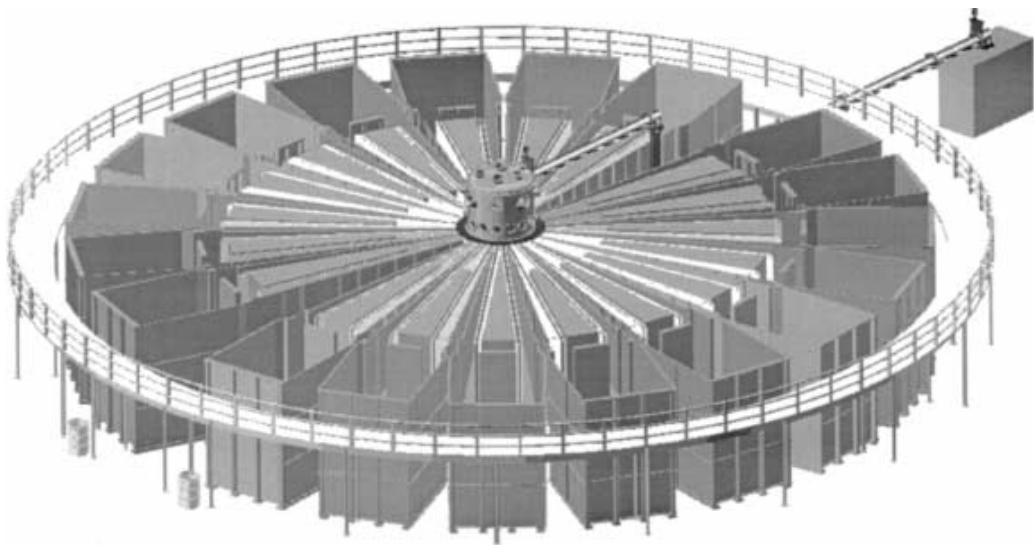


Figure 1. Design view of Atlas.

The 36-MJ Atlas capacitor bank will consist of 152 Marx modules, each containing four, 60-kV capacitors. Two closing switches will be used to “erect” each of the Marx modules into its 240-kV configuration. The capacitors in an individual module will be interconnected with a stainless steel resistor to provide damping. High-voltage coaxial cables will be used to transmit current

from four of these modules to an output isolation switch. The other side of the output isolation switch will be connected to an oil-insulated tri-plate transmission line. A total of 38 of these lines will converge on to a central header which surrounds the target chamber. A schematic of a 240-kV Marx module is shown in Fig. 2.

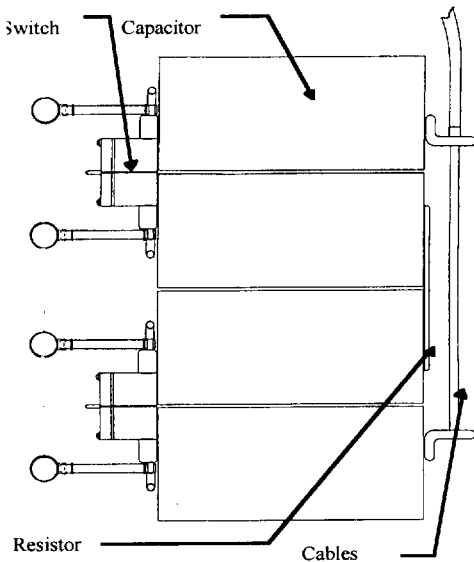


Figure 2. 240-kV Marx module

The 240-kV modules will be arranged in vertical stacks with two modules in each stack. For fast opening switch development, the two modules can be connected in series to form a single 480-kV Marx module. This reduces the rise time of the system and therefore the time the switch is required to conduct current in a “closed” state. Two stacks of two Marx modules will form a “maintenance unit”. Each maintenance unit will be independently removable from the system and will contain its own control and data acquisition module and railgap trigger system. Railgap periodic maintenance requirements indicate that one maintenance unit will be removed from the system for refurbishing after each major test. The modularity of the maintenance units will help achieve the anticipated repetition rate of 2 shots/week while still maintaining the overall system reliability requirements.

Atlas capacitor design is based on the 15% voltage-reversal, 30-kJ capacitors used in the Pegasus Facility. Each Atlas capacitor is rated at 60-kJ stored energy (two 30-kJ Pegasus II units in parallel), 60-kV charge voltage, 330-kA discharge current, and less than 20-nH inductance. The case style has been modified to a *Fastcap*⁶ configuration which will greatly ease the construction of the Marx modules. These cases are fiberglass with electrical bushings mounted at the front and rear of each capacitor. Capacitors from two vendors are currently under evaluation to certify their performance capabilities under Atlas operating conditions.

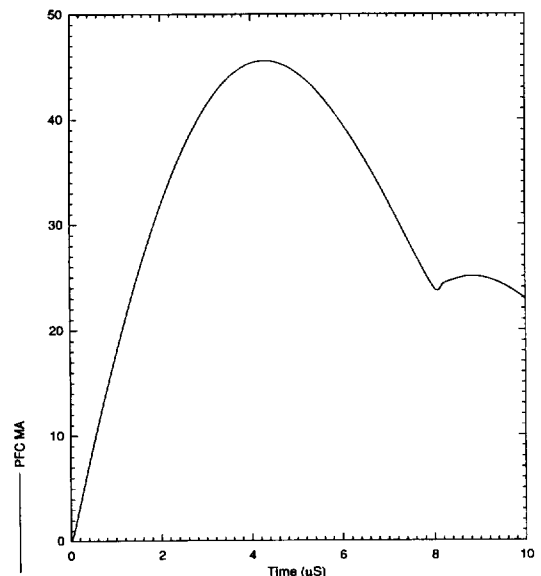


Figure 3. Atlas liner current for a 68-gm liner at 240-kV.

Figure 3 shows a simulation of the Atlas current waveform driving a 5.3-cm radius, 68-gm aluminum liner. As can be seen from the illustration, a peak liner current of 45 MA is reached in 4.3-μs.

Each of the 300 switches in the Atlas system will be operated at a 120-kV holdoff voltage, a 330-kA conduction current, and a 3-coul charge transfer. We chose the railgap switch for this application because of its demonstrated low jitter, low inductance, and high coulomb-transfer capabilities in other pulsed power systems.⁷ We tested several of these switches in the laboratory at current levels exceeding 800-kA and at a charge-transfer exceeding 5-coulombs. The switch performed well with the exception of deformation of the trigger rail under prefire conditions. We are presently working with the manufacturer to improve its mechanical integrity. Our tests indicate that after approximately 400- to 500-coul of accumulated charge transfer, the switch will prefire at 120-kV. For an individual switch to have a prefire probability of less than 10^{-4} , periodic maintenance will be required approximately every 240 coulombs.

There will be two types of damping resistors in the Atlas system. Series resistors, which must conduct the full discharge current of each module, are used to limit the voltage reversal on the capacitors. We are now testing a folded stainless steel foil resistor for this application. The other type of damping resistor is a shunt resistor and is used to absorb high-frequency, parasitic oscillations between Marx modules and the header system. The shunt resistors will be located across the output of each module and are only required to conduct modest currents.

Target Chamber

Present estimates indicate more than 12-MJ of energy will be trapped and dissipated in the target chamber when the vacuum insulator breaks down from the Poynting vector changing direction. The current design of the target chamber has walls that are lined with energy absorbing material to prevent damage from the shrapnel and debris of the discharge. The chamber will be approximately 2 m in diameter to support the extensive suite of diagnostics that is anticipated.⁸

A high degree of flexible diagnostic access is necessary to accommodate the wide variety of proposed experiments. Diagnostic access for end-on and radial views of the target will be available. Several in-line port pairs for diagnostics that involve active backlighting with visible light or x-rays will also be available. The large chamber dimensions necessitate re-entrant port capability for those diagnostics that require high flux. To facilitate alignment of these diagnostics, the target chamber and associated diagnostics will be preassembled in a staging area and then lowered onto the machine for final alignment.

Experimental Capabilities

The principal applications of Atlas are hydrodynamics and material properties studies under extreme conditions. Most of these applications rely upon the ability of Atlas to implode heavy liners at high velocity. The experimental requirements we place upon heavy liner performance are that: 1) the inner surface of the liner attain high velocity, with 2) smooth uniform drive, while 3) the inner surface remains unmelted. These conditions are required for many experiments in which the initial conditions of the inner liner surface must be accurately known. For the Atlas

drive conditions, a standard liner has been designed to achieve these conditions; its dimensions are shown in Figure 4. Starting at a radius of approximately 5 cm, this liner accelerates to a velocity of 20 km/s at a radius of 1 cm. As shown in the plot in the inset, 1D MHD calculations show that at peak velocity, the inner surface is still at room temperature.

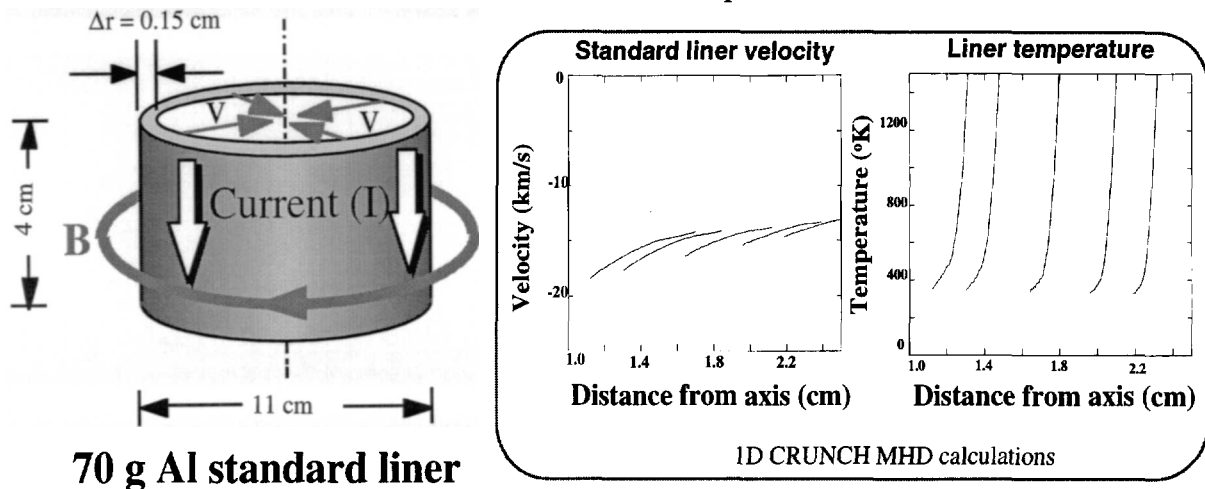


Figure 4. Dimensions of the standard aluminum liner, optimally designed for Atlas drive conditions. The inset shows liner velocity and temperature profiles in the liner, calculated with the 1D MHD Crunch code. The liner inner velocity approaches 20 km/s, while the inner surface remains unmelted.

Figure 5 summarizes some of the conditions achievable with Atlas liner implosions, using various types of interior target geometries. For the most part, these conditions cannot be achieved by any other technique. A large number of experiments may be performed in these environments, including equation of state, particle transport, instability growth, mixing in convergent geometries, hydrodynamic flows in complex structures, and magnetized target fusion.⁹

Experimental Environment	Conditions Achievable
Shock compression	$P > 2.5 \text{ TPa (25 Mbar)}$
Quasi-adiabatic compression	$\rho/\rho_0 > 6$ (for heavy metals), $P > 100 \text{ Mbar}$
Strongly coupled plasmas	$\Gamma > 30$, $\Theta > 1$
Magnetic field (axial)	$B \sim 2000 \text{ T}$
Strain and strain rate (shockless)	$\epsilon > 200\%$, $d\epsilon/dt \sim 10^4 - 10^6$
Material instability	Nonlinear & turbulent regimes, multi-cm
Velocity	$v > 20 \text{ km/s}$ with unmelted inner surface

Figure 5. High energy-density experimental environments achievable with Atlas.

In order to perform experiments under these conditions, a comprehensive suite of diagnostics is planned. The workhorse diagnostic for many experiments will be radiography, especially multi-view flash radiography driven by miniature pulsed power sources.¹⁰ Implementation of a laser x-ray backlighting capability is also being studied. Interferometry, shadowgraphy, holography and

streaked and gated imaging will be available for imaging surface structures, spallation effects, and instability growth. VISAR and fiber-optic pin arrays will be used for precision velocity measurements. Time-resolved infrared and optical pyrometry will be used for measuring the relatively low-temperature histories associated with high strain-rate and melting phenomena. For the higher temperatures produced in dense plasmas, soft x-ray spectroscopy will be used. The pressure-dependent Raman shift in diamond is being developed as a pressure diagnostic in the multi-megabar regime.¹¹ Dense plasma and time-dependent neutron diagnostics will also be fielded for magnetized target fusion experiments. In many cases, Pegasus II is being used as a testbed for developing the diagnostics needed for Atlas.¹²

Since a review of all proposed experiments is beyond the scope of this paper, we will discuss two types of Atlas experiments here. These are Hugoniot measurements in heavy metals and studies of non-degenerate, strongly-coupled plasmas. Figure 6 shows a conceptual experimental layout for measuring the principal Hugoniot.

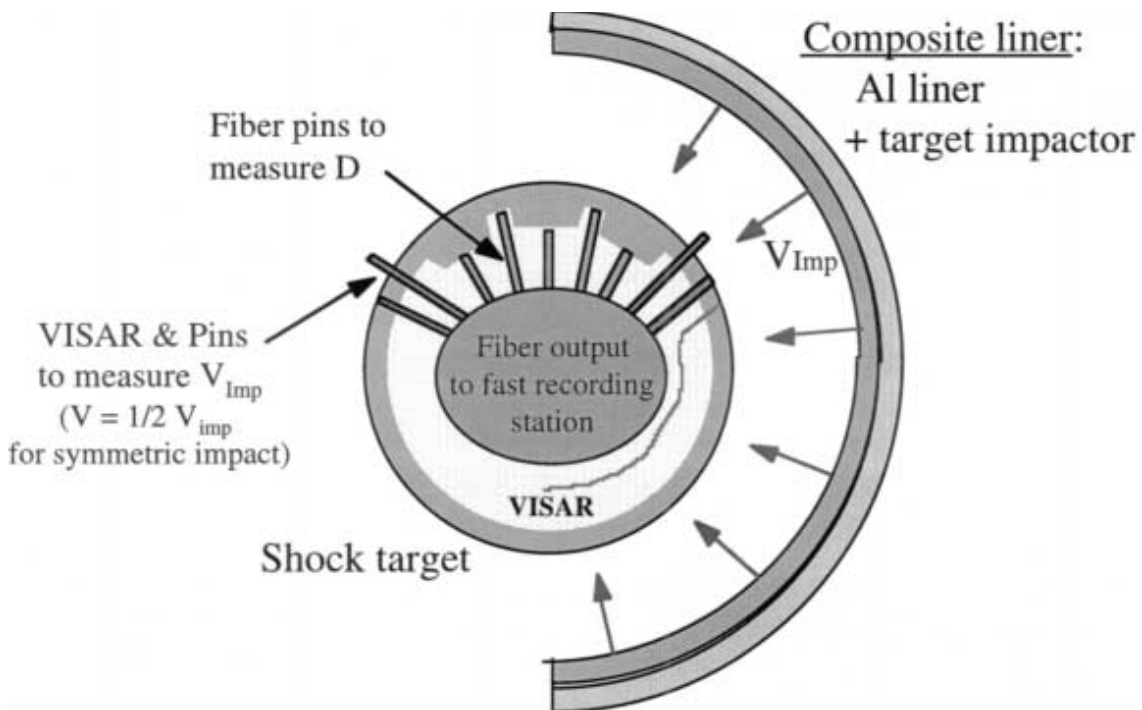
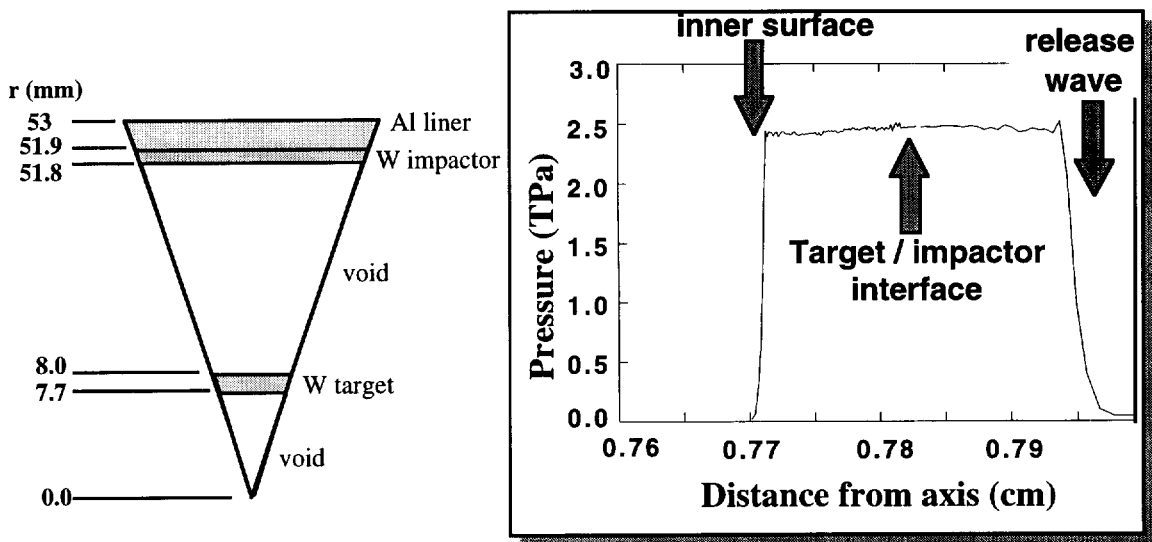


Figure 6. Conceptual experimental configuration for a direct Hugoniot measurement using Atlas. Measurement of impactor velocity and shock velocity across steps on inner target surface yield a direct determination of the equation of state (pressure, density, and internal energy) of the shocked material.

A composite liner is composed of an Al outer layer and a dense inner layer. The Al shell is used primarily to carry current, while the inner layer serves as the target shock impactor. An inner cylinder of target material is placed at the center of the liner. Interior to the target cylinder is the diagnostic package. Load dimensions and results of a 1D MHD simulation for a tungsten

Hugoniot experiment are shown in Figure 7. In this case, a 1.4 cm diameter hollow core on axis provides adequate room for deploying fiber optics for shock detection pins and an imaging VISAR system. Target and liner thicknesses are chosen so that 1) release waves from the Al-W interface do not overtake and attenuate the shock before a shock velocity measurement can be made, and 2) the target thickness is large enough to allow an accurate measurement (i.e., ~1% or better) of the shock transit time.

Figure 7 shows that when the liner impacts the target, a steady 2.5 TPa (25 Mbar) shock is produced in the W target. We measure two quantities in this experiment, the shock propagation speed, D , and the impactor velocity, V_{imp} . $D = \Delta x / \Delta t$ is determined by measuring the transit time Δt across accurately measured steps ($\Delta x = 0.2\text{-}0.3$ mm thick) on the inner target surface, using fiber optic shock arrival detectors. The impactor velocity is measured either with pins or VISAR, also with an accuracy of ~1%. Because the impact involves similar materials, conservation of momentum requires that the particle speed, V , behind the shock front is identically equal to $V_{imp}/2$. Invoking this equality depends critically upon the criteria that the liner surface is smooth and not preheated.



impactor velocity = 18 km/s

1D Crunch calculation of pressure pulse near inner surface of tungsten target

Figure 7. Target design for a 2.5 TPa (25 Mbar) Hugoniot experiment in tungsten.

Shock pressure, density, and internal energy are calculated directly from the measured values of D and V , using the well-known Rankine-Hugoniot relations. We note that experiments of this type can significantly extend the range of direct, accurate Hugoniot equation of state measurements. The pressure of 25 Mbar should be compared to values of <10 Mbar, achievable with two-stage light-gas guns.¹³ Although pressures in the 25 Mbar range are readily achieved

with high-energy pulsed lasers, no direct measurements on metals have been made to date, due to the difficulty in measuring V in non-impact shock experiments.

Atlas will also be a testbed for strongly coupled plasma experiments. Such experiments fall into three categories: fundamental physical property measurements (e.g., equation of state and transport properties), basic hydrodynamic experiments (e.g., Richtmyer-Meshkov instability growth in a dense plasma), and hydrodynamics in complex structures (e.g., through gaps and cracks, around discontinuities, etc.).

We are especially interested in strongly-coupled, partially degenerate plasma systems. These are systems in which ion-ion interactions are strong relative to thermal excitations, yet the temperature is significant compared to the Fermi energy. In the simplest description such plasmas are characterized by two parameters, Γ and Θ . $\Gamma = (4\pi/3)^{1/3} Z^2 e^2 / kT$, where Z is the degree of ionization, measures the relative magnitude of the Coulomb potential between two ions compared to kT . When $\Gamma > 1$, a plasma is said to be strongly coupled. Of course, room temperature metals all have $\Gamma > 1$. Low temperature metals, however, are degenerate electron systems (i.e., $kT \ll E_F$, the Fermi energy) and are described by Fermi-Dirac statistics. Most interest pertains to electron systems at higher temperature (i.e., $\Theta = kT/E_F > 1$), for which the electrons are at least partially described by Maxwellian statistics. Plasmas for which $\Gamma > 1$ and $\Theta > 1$ present a great challenge to theoretical physics, since neither descriptions based upon standard plasma physics models (in which $\Gamma \ll 1$ is assumed) nor condensed matter physics models (in which $\Theta \ll 1$ is assumed) can be applied in a straightforward way. Unfortunately, very little experimental data in this regime exists. Consequently, the material properties of strongly-coupled, partially degenerate plasmas are considered to be known only with a high degree of uncertainty. These uncertainties strongly affect modeling of hydro in such systems.

Several experimental geometries for strongly coupled plasma experiments are being considered for Atlas, embracing the three categories of experiments mentioned above. Figure 8 shows a geometry that might be used for measuring equation of state or electron transport of a strongly-coupled, partially degenerate plasma. In this experiment, a liner is imploded onto a target assembly consisting of a low-density preheated plasma confined between high-density cylinders (anvils). The preheated plasma is produced by using a relatively small (~few hundred kJ) auxiliary capacitor bank to explode a wire array into a plasma that fills the volume between the anvils. The liner impact produces a strong shock that reverberates many times between the anvil walls, ringing the target plasma up to high pressure.¹⁴ Using a combination of shock arrival measurements, radiography, and energy balance, we should be able to obtain the EOS of the target plasma.

- Conditions at 10.3 μ s*
(from 1D Crunch calculations)
- $\rho = 27 \text{ g/cm}^3$
 - $T = 23 \text{ eV}$
 - spatially uniform over $\sim 1 \text{ mm}$
 - conditions stable for $\sim 1 \mu\text{s}$ before disassembly

$\Gamma \simeq 30, \Theta \simeq 1.0$

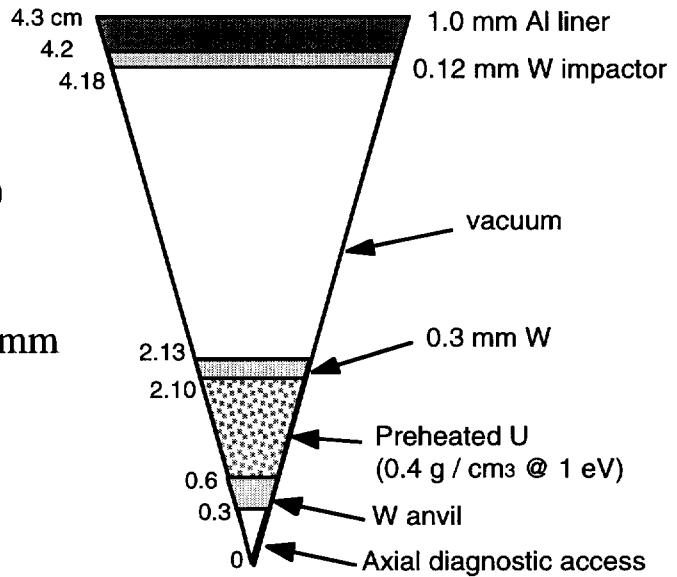
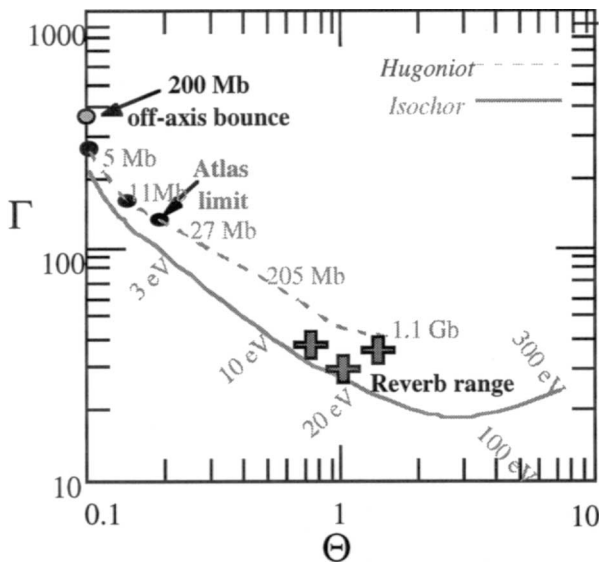


Figure 8. Liner-target configuration for a producing strongly-coupled, partially degenerate uranium plasma. Calculations were performed with the CRUNCH 1D.

A target design for producing a strongly coupled uranium plasma is shown in Figure 8. A $\sim 10 \text{ g U}$ exploding wire plasma reaches a density of $\sim 0.4 \text{ g/cm}^3$ and a temperature of $\sim 1 \text{ eV}$



before shock reverberation. The shock produces a final state in the uranium of $\sim 27 \text{ g/cm}^3$ and 23 eV . This state is spatially uniform throughout the plasma (about 1 mm thick) and persists for $\sim 1 \mu\text{s}$, favorable conditions for making measurements. Figure 9 shows the values of Γ and Θ that are achieved for three slightly different target geometries. We see that the U plasma has $\Gamma \sim 30$ and $\Theta \sim 1$. These conditions cannot be achieved through exploding wire techniques, and, as shown in Figure 9, can only be reached by direct shock compression for pressures of order 1 Gbar .

Figure 9. Values of Γ , the plasma parameter, and Θ , the electron degeneracy parameter, calculated for uranium in various experimental high energy-density environments. The 1D MHD code, CRUNCH, was used to calculate the reverberation results (shown as crosses) and the 200 Mbar bounce of a dense liner off the axis. The Hugoniot and isochor were determined from the Los Alamos SESAME EOS library. For all calculations, a Thomas-Fermi model was used to calculate the degree of ionization.

References

- ¹ Presidential Decision Directive and Act of Congress (P.L. 103-160).
- ² "The Stockpile Stewardship and Management Program: Maintaining Confidence in the Safety and Reliability of the Enduring U.S. Nuclear Weapon Stockpile", U.S. Department of Energy, Office of Defense Programs, May 1995.
- ³ J.C. Solem, "Basic Science with Pulsed Power & Some Off-the-Wall Ideas", LA-UR-95-1110, presented at the *Spring Workshop on Basic Science Using Pulsed Power*, Santa Barbara, CA, April 5-7, 1995.
- ⁴ D.D. Bloomquist, et. al., "Saturn: A Large X-Ray Simulation Accelerator", *Proc. 6th IEEE Int'l. Pulsed Power Conf.*, pp 310, June, 1987.
- ⁵ R.B. Spielman, et. al., "Pulsed Power Performance of PBFA-Z, *Proc. 11th IEEE Int'l. Pulsed Power Conf.*, these proceedings.
- ⁶ W.A. Reass, et. al., "Capacitor and Railgap Development for the Atlas Machine Marx Modules", *Proc. 10th IEEE Int'l. Pulsed Power Conf.*, pp 522, July, 1995.
- ⁷ R.E. Reinovsky, et. al., "Shiva Star Inductive Pulse Compression System", *Proc. 4th IEEE Int'l. Pulsed Power Conf.*, pp 196, June, 1983.
- ⁸ G. A. Wurden, et al., "Atlas Chamber and Diagnostic Interface Design," *Proc. 11th IEEE Int'l. Pulsed Power Conf.*, these proceedings.
- ⁹ I. Lindemuth, et al., "Mago/MTF: Controlled Thermonuclear Fusion With Existing Pulsed Power Systems?", *Proc. 11th IEEE Int'l. Pulsed Power Conf.*, these proceedings.
- ¹⁰ N. S. P. King, et al., "Performance of the Multi-Pulse X-Ray Imaging System for the Pulsed Power Hydrodynamic Experiments at LANL," *Proc. 11th IEEE Int'l. Pulsed Power Conf.*, these proceedings.
- ¹¹ G. Rodriguez, et al., Development of a High Pressure Diagnostic Based On Optical Raman Backscatter Measurements in Diamond," *Proc. 11th IEEE Int'l. Pulsed Power Conf.*, these proceedings.
- ¹² J. S. Shlachter, et al., "Pegasus II Experiments and Plans for the Atlas Pulsed Power Facility," *Proc. 11th IEEE Int'l. Pulsed Power Conf.*, these proceedings.
- ¹³ L. M. Barker, et al., in *High Pressure Shock Compression of Solids*, (New York: Springer-Verlag, 1992), p. 47.
- ¹⁴ This technique is similar to that discussed by S. T. Weir, et al., *Phys. Rev. Lett.* **76**, p. 1860 (1996).